

Numerical Study of Particle Flow and Solar Radiation Transfer in CPC Photocatalytic Reactor for Hydrogen Production: A Case Study

Jiafeng Geng ^{1,2}, Qingyu Wei ³, Bing Luo ^{1,4}, Shichao Zong ^{1,2}, Lijing Ma ⁴, Yu Luo ^{4,*},
Chunyu Zhou ^{1,2,*}
and Tongkun Deng ²

¹ Key Laboratory of Subsurface Hydrology and Ecological Effects in Arid Region of the Ministry of Education, Chang'an University, Xi'an 710054, China; gengjf@chd.edu.cn (J.G.); shichaozong@chd.edu.cn (S.Z.);

² School of Water and Environment, Chang'an University, Xi'an 710054, China; deng17870061003@outlook.com

³ Beijing Aerospace Propulsion Institute, Beijing 100191, China; wei.1203@stu.xjtu.edu.cn

⁴ International Research Center for Renewable Energy, State Key Laboratory of Multiphase Flow in Power Engineering, Xi'an Jiaotong University, Xi'an 710049, China; ljma@mail.xjtu.edu.cn; luobing@xjtu.edu.cn

* Correspondence: 13289367808@163.com (Y.L.); zhouchy@chd.edu.cn (C.Z.); Tel.: +86-02982339965 (Y.L. & C.Z.)

S1. The Basic Principles of CPC

S 1.1 Parametric Equations of CPC

A compound parabolic concentrator (CPC) is a type of optical device used to efficiently collect and focus light onto a specific target. It consists of multiple parabolic reflectors arranged in such a way that incoming light undergoes multiple reflections and refractions within the concentrator, ultimately converging at a focal point or line. This design allows for the concentration of light over a wide range of angles, making CPCs particularly useful for applications such as solar energy harvesting, optical communications, and photovoltaic systems. The compound parabolic shape helps minimize optical losses and maximize the collection efficiency, making CPCs a versatile and effective tool in various optical and photonic systems.

Figure S1 depicts a sectional diagram of the CPC with a tubular absorber. It consists of two parabolas (BM and CN) and two involutes (PM and PN). Since the cross-section of the receiving tube is circular, the two parabolas are extended along involutes corresponding to the circular cross-section of the receiving tube (as any light incident on the involute can be reflected to the base circle surface, achieving light convergence). The parametric equations for the curves are as follows:

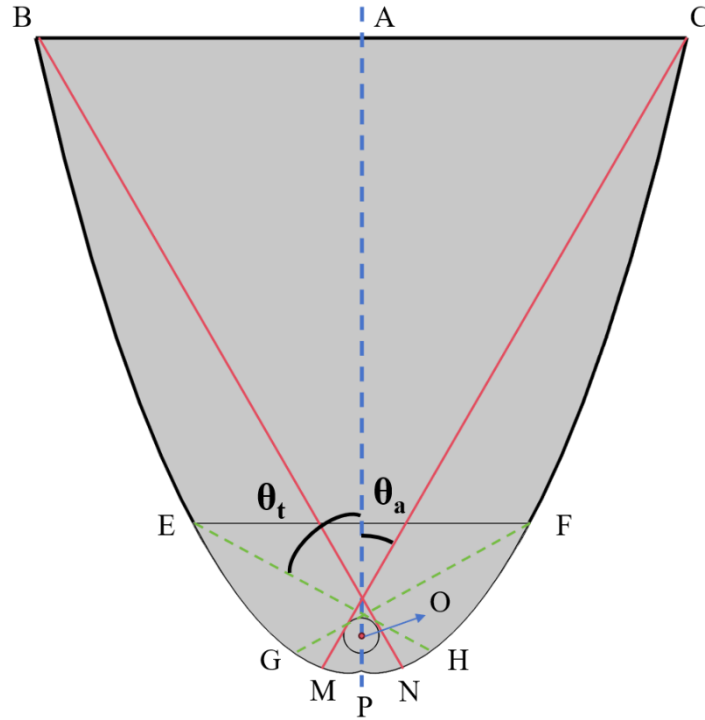


Figure S1. schematic diagram of the CPC section

For the involute curve PN in the Figure S1:

$$X = r_b \sin t - I(t) \cos t \quad (\text{S-1})$$

$$Y = -r_b \cos t - I(t) \sin t \quad (\text{S-2})$$

$$\cos t_0 = r_b / (r_b + Gap) \quad (\text{S-3})$$

$$I(t) = \sqrt{(2r_B \text{Gap} + \text{Gap}^2)} + r_B(t - t_0) \quad (\text{S-4})$$

where the t is the parameter, and the range of it is: $t_0 \leq t \leq \pi / 2 + \theta_a$

For the parabola curve NC in the Figure S1:

$$X = r_B \sin t - I(t) \cos t \quad (\text{S-5})$$

$$Y = -r_B \cos t - I(t) \sin t \quad (\text{S-6})$$

$$\cos t_0 = r_B / (r_B + \text{Gap}) \quad (\text{S-7})$$

$$I(t) = \frac{2(\sqrt{(2r_B \text{Gap} + \text{Gap}^2)} - r_B t_0) + r_B [\pi/2 + \theta_a + t - \cos(t - \theta_a)]}{1 + \sin(t - \theta_a)} \quad (\text{S-8})$$

where the range of parameter t is: $\pi / 2 + \theta_a \leq t \leq 3\pi / 2 - \theta_t$

S 1.2 Introduction to ray tracing method and determination of intensity

As has been described in the main text, the ray tracing method solves for the position and wave vector of individual rays. In brief, the ray tracing method involves emitting a certain number of rays in the model to represent incident light, and then allowing these rays to propagate through the medium according to the laws of geometric optics and interact with the boundaries. Additionally, every time the intersection of a ray with a surface is detected, a wide variety of ray-boundary interactions may apply. These include specular reflection, diffuse reflection, refraction, and several different types of absorption.

In ray tracing methods, the intensity computation is also performed using discrete methods. That means that every ray is treated as a small point source, which contains a certain amount of radiation. And then the energy contained in the rays could be cumulated in each mesh element. Next, divide the accumulated radiation energy within each mesh element by the area of the element to obtain the radiation intensity. With this method, the distribution of the radiation intensity on the surface can be obtained.

S 1.3 Analysis of the optic efficiency of CPC

The optical efficiency of the CPC can be evaluated from the perspective of energy received. Following the method described in the previous section, integrating the radiation intensity on the receiving tube surface yields the total radiation energy received, and the ratio of the radiation energy received on the surface of the receiving tube and the total radiation energy arrived at the CPC is the concentrating efficiency of the CPC.

According to this method, it can be observed that the concentrating efficiency of CPC varies under light incidence at different angles, as shown in Figure S2 and Table S1.

Table S1 List of the concentrating efficiency under different incident angle

	0°	15°	30°	45°	60°
Concentrating efficiency	100%	28.4%	16.6%	14.8%	0%

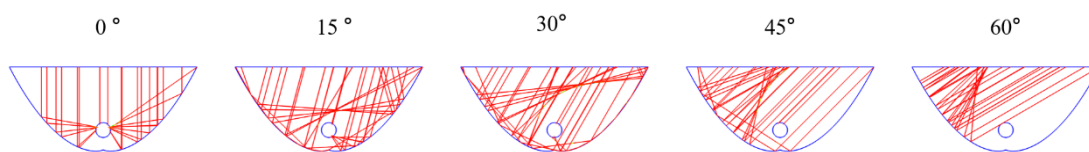


Figure S2. schematic diagram of the different incident angle on CPC

As seen from the Figure S2 and Table S1, the concentration efficiency of CPC reaches its maximum at an incident light angle of 0° , corresponding to vertical incidence, which is 100%. With an increase in the incident light angle, the concentration efficiency gradually decreases, until it reaches 0% at larger incident angles. Therefore, in practical applications, if CPC is used in a tracking mode where the entrance of the CPC is always perpendicular to the sun, the maximum concentration efficiency can be achieved. However, considering operational costs, intermittent operation modes are also commonly used. For instance, in the experimental platform mentioned in our previous work, an intermittent operation mode was adopted, with a 5° adjustment every hour [22].

In our case study, the model was constructed and simulated based on the position of the CPC and the direction of the sun at noon. Since the CPC is not perpendicular to the direction of direct solar radiation, the concentration efficiency cannot reach 100% at this time. This setup aligns with actual operational parameters. Additionally, it should be noted that the radiation reflected after CPC reflection and not directly absorbed by the receiving tube can escape, and scattering by the catalyst can also cause light to escape. These escaped rays can be considered for applications such as adding secondary concentrating devices, but their economic feasibility also needs to be evaluated.

S2. Brief introduction of the experimental platform

As has been mentioned in the main text, we designed and developed a direct solar photocatalytic water splitting system for hydrogen production in our previous research work, which is shown in Figure S3[22]. The system consists of low-precision tracking concentrator arrays, 19 parallel reaction lines with single length of 2.0–2.7 m and gas pulse perturbation control. The central solution tower is used to provide the high liquid level difference, gas-liquid-solid separation and heat exchanger control. The distribution, collection pipelines and other basic hardware components are used in the system. The light receiving and the reaction medium circulation are significantly improved in the system. The outlet gas of the system is connected to a wet gas meter to measure the amount of hydrogen. The solar irradiation meter (TBQ-4-6, 260–3000 nm, precision: $\pm 2\%$) is used to measure the irradiation intensity of the incident to the CPC plane. The volume of reaction solution is 720 NL, the photocatalyst ($\text{NiS-Cd}_x\text{Zn}_{1-x}\text{S}$) concentration is 0.25 g/L and the concentrations of the sacrificial agents are 0.25 mol/L Na_2SO_3 and 0.35 mol/L Na_2S .

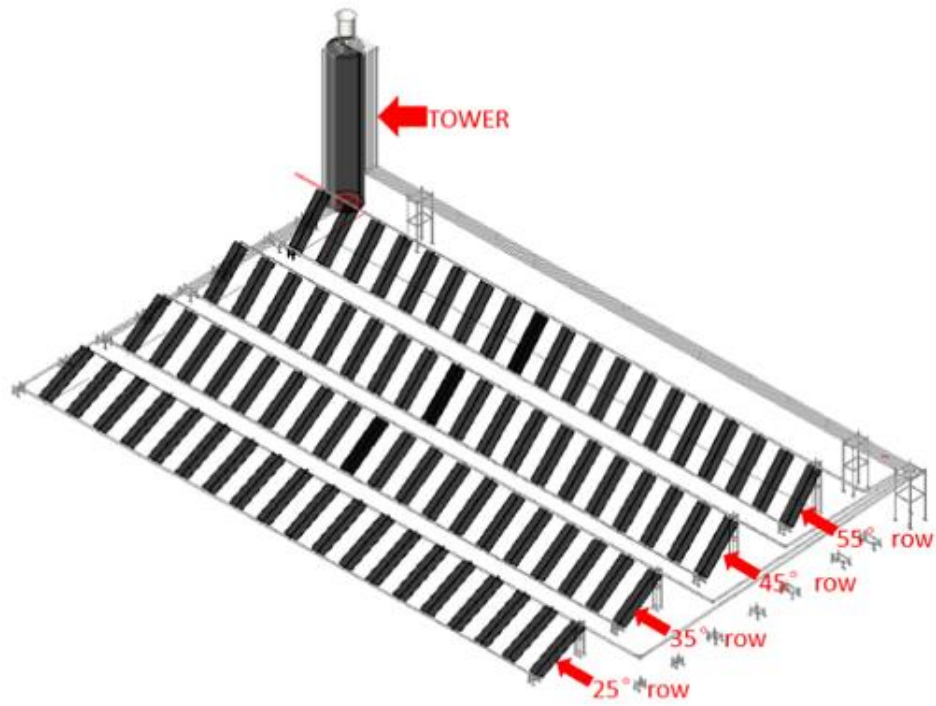


Figure S3 The outdoor layout of the designed system with three-dimensional perspective. [22]